Eur. Phys. J. B **43**, 175–185 (2005)
DOI: 10.1140/epjb/e2005-00040-8

THE EUROPEAN PHYSICAL JOURNAL B

Theory of neutron scattering for gapless neutral spin-1 collective mode in graphite

S.A. Jafari[1,2,a] and G. Baskaran[2]

[1] Department of Physics, Sharif University of Technology, Tehran 11365-9161, Iran
[2] Institute of Mathematical Sciences, Madras 600 113, India

Received 1st September 2004
Published online 25 February 2005 –

Abstract. Using tight binding band picture for 2D graphite, and the Hubbard interaction, recently we obtained a gapless, neutral spin-1 collective mode branch in graphite [Phys. Rev. Lett. **89**, 016402]. In this paper we present a detailed RPA analysis of the Neutron Scattering cross section for this collective mode. Near K-point and very close to Γ-point, the intensity of neutron scattering peaks vanishes as q^3. This is shown using a simple Dirac cone model for the graphite band structure, which captures the small-q behavior of the system. As we move away from the Γ- and K-points in the Brillouin zone of the collective mode momenta, we can identify our collective mode quanta with spin triplet excitons with the spatial extent of the order of a few to a couple of lattice parameter a, with more or less anisotropic character, which differs from point to point. We also demonstrate that the inclusion of the long range tail of the Coulomb interaction in real graphite, does not affect our spin-1 collective mode qualitatively. This collective mode could be probed at different energy scales by thermal, hot and epithermal neutron scattering experiments. However, the smallness of the calculated scattering intensity, arising from a reduced form factor of carbon $2p_z$ orbital makes the detection challenging.

PACS. 71.10.Li Excited states and pairing interactions in model systems – 78.70.Nx Neutron inelastic scattering

Introduction

Graphite is a broad band tight-binding system composed of hexagonal graphene sheets held together by van der Waals interaction. This pure carbon system, in spite of a simplicity in electronic and crystal structure, has a rich physics and continues to surprise us [1]. The four valence of each carbon atom is used to form σ and π bonds with its three neighbors. Novoselov et al. have been able to prepare an atomically thin layer of carbon in the laboratory [2], paving way for new directions in experimental studies. Each such a layer is like a giant molecule with resonating π bonds among many valence-bond configurations [3]. This structure is similar to many interesting systems such as carbon nano-tubes, buckyball, MgB_2 etc. Within each graphene layer, p_z electrons of each carbon atom can hop from a site to another site. These electrons are responsible for the formation of π bands which touch each other at the corners of the Brillouin zone (Fig. 2).

An important question is to understand the nature of low energy collective excitations in our zero gap planar $p-\pi$ bonded graphite. We may approach this question in an unconventional fashion starting from organic chemistry! Planar $p-\pi$ bonded molecules form the basis of organic chemistry, benzene being a first member. Benzene is a mini-graphite in some respects. One can also view graphite as an end member of planar $p-\pi$ bonded molecules – benzene, naphthalene, anthracene, coronene etc. It is well known [4] that benzene and the above sequence have a spin triplet state as their first excited state. The next excited state is a singlet state nearly 2 eV above the triplet state for benzene. This remarkable singlet-triplet splitting, which is missing in simple Huckel theory, is a well known effect of coulomb correlation in $p-\pi$ bonded systems.

A natural question is what happens to the triplet and singlet excitons in graphite, the end member of the above sequence. In a recent paper we showed that in graphite the triplet excitons form a well defined band in the entire Brillouin zone [5]. We view the low energy part of the above exciton as a spin-1 collective mode in view of its gapless character. The singlet excitons, on the other hand form the well known π plasmon (energy ~ 7 eV) with a finite gap in the spectrum. Since graphite is also viewed as a semi-metal, our neutral spin-1 collective mode can be also viewed as Landau's 'Spin-1 Zero Sound' (SZS).

[a] e-mail: akbar@imr.edu

Another way to understand the low energy collective mode in graphite is to go back to Pauling's resonating valence bond (RVB) theory of graphite [3]. Pauling assumed a dominant near neighbor singlet $p-\pi$ bonds and their resonance to develop a theory of graphite. We know from recent developments in RVB theory that such a well developed singlet correlation leads to a quantum spin liquid state. A quantum spin liquid state either has a collective spin-1 branch or contains spin-half spinon excitations by quantum number fractionization. Our finding of a gapless spin-1 mode qualifies graphite to be a quantum spin liquid state. The gapless character of the spin-1 branch, however, makes it a long range RVB state rather than a short range RVB state as envisaged by Pauling.

Yet another physical picture of our spin-1 collective mode is as follows. In graphite the valence band is completely filled and the conduction band is completely empty. The nature of particle-hole continuum in this system is such that a window below the particle-hole continuum opens (see Fig. 4). A Hubbard type on site repulsion between the electrons is in the spin singlet channel. This translates into an attraction in particle-hole spin triplet channel. This can bind an electron and a hole into a spin-1 exciton; this appears as a pole for the spin susceptibility inside the window which exists below the particle-hole continuum. There are special band structure reasons as to why our spin-1 excitations are gapless, which will be explained in detail below. Use of the short range interaction for the spin phenomena is justified, since (as in the following we will explicitly demonstrate for the case of spin-1 collective mode) inclusion of the long range tail of the interaction does not affect the spin physics qualitatively.

Gapless spin-1 excitation (Goldstone modes) are characteristic of magnetically ordered systems. In the now popular case of La_2CuO_4, a 2D quantum antiferromagnet, the spin-wave bandwidth is of the order of $\sim$100 meV. But in the case of graphite, which has no long range magnetic order, this gapless spin-1 collective branch (a non-Goldstone mode) has a wide dispersion $\sim 0-2$ eV (Fig. 5). This energy range should be compared with triplet exciton of buckyball at $\sim$1.64 eV [6]. Spin-1 collective mode of graphite exists everywhere in BZ and since it does not enter the particle-hole continuum, is protected form Landau damping (decaying into particle-hole pairs). Therefore the spin-1 collective mode of graphite is long-lived and could be exploited in coherent transport of spin-only (neutral) currents through the nano-tubes.

Since the bandwidth of this collective mode is very large, each energy range should be investigated by different probe. Here we will concentrate on inelastic neutron scattering experiments. In real graphite, there are very small electron-hole pockets around the K-points of the order of $\sim 10-20$ meV; they arise from including hopping and spin-orbit coupling effects. Above this energy range, the collective mode is well isolated from the typical phonon energies and therefore the neutrons need not to be polarized. The low energy parts (regions close to Γ-point in Fig. 5) of the collective mode up to $\sim$100 meV can be probed with thermal neutrons. Hot neutrons can concentrate on higher energies $\sim 100-500$ meV (around the Γ-point). The highest energy parts $\sim$0.5 eV-up-wards (regions midway between $\Gamma-M$ and midway between $\Gamma-K$) correspond to bound state wave function with spatial extent of the order of a few unit cell ($\sim$2 Å) and can be studied by hot and/or epithermal neutrons.

However, an important practical difficulty is the small value of scattering cross section. As we will see in detail, the large size of the spin carrying $2p_z$ orbital of carbon reduces the neutron scattering form factor significantly, making $S(\mathbf{q},\omega)$ rather small in relevant regions in $(\mathbf{q},\omega)$ space. A most appropriate region, where experiment have better chance for discovering the spin-1 mode is in the region midway between the Γ and M points in the Brillouin zone.

In this paper we present the detailed RPA analysis of the spin susceptibility and the neutron scattering cross section. The bare value of Hubbard U in graphite is $\sim$8 eV, but the renormalized value for stability issues, should be less than $2.23t \sim 5.8$ eV. We will keep U as a parameter to be determined by experiment and will report the results of cross section calculation for $U \sim 5$ eV. The organization of the paper is as follows. We begin with a review of band picture of graphene which is essential for understanding the nature of the window below the particle-hole continuum. The RPA formulation of the next section is applied to tight-binding bands of graphene in later sections. To get an analytical handle, we exactly obtain the spin susceptibility within the RPA for model of a single Dirac cone. This model captures the behavior near the Γ and K-point. We calculate the intensities of the neutron scattering peaks for the linearized model and also discuss the effect of including long range tail of the interaction. Finally we report the numerical calculation of the intensities of the neutron scattering peaks for entire BZ along with calculation of the real space profile of the excitonic wave-function. To be self-contained, in Appendix A, we review excitonic formulation of the problem.

The tight-binding band structure

Within the tight-binding approximation, and neglecting the overlap between the $2p_z$ atomic orbitals of neighboring carbon atoms, the band dispersion of graphene is given by $\varepsilon^{c/v}_{\mathbf{k}} = \pm t\ \varepsilon_{\mathbf{k}}$ where

$$\varepsilon_{\mathbf{k}} = \sqrt{1 + 4\cos\left(\frac{\sqrt{3}k_x a}{2}\right)\cos\left(\frac{k_y a}{2}\right) + 4\cos^2\left(\frac{k_y a}{2}\right)} \tag{1}$$

where $+$ and $-$ signs correspond to conduction and valence bands, respectively [11,10]. Here a is the length of translation vector in one of the sub-lattices of graphene: $a = \sqrt{3}\times$(C-C bond length) as depicted in Figure 1. The above bands touch each other at the K-points (corners) of the BZ as depicted in Figure 2. Figure 3 shows the DOS corresponding to the dispersion (1).

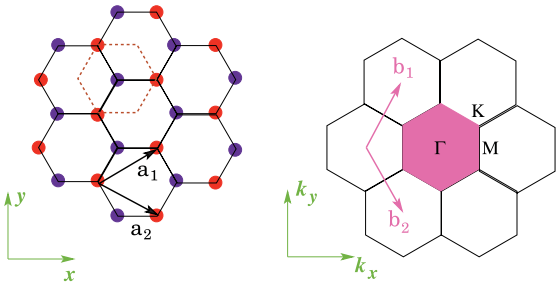

Fig. 1. (left) Lattice structure of a two-dimensional graphene sheets. It is a bipartite lattice composed of two sub-lattices. Each sub-lattice is denoted by a different color. The basis vectors of real space lattice are given by $\vec{a}_1 = \frac{\sqrt{3}a}{2}\hat{e}_x + \frac{a}{2}\hat{e}_y$, $\vec{a}_2 = \frac{\sqrt{3}a}{2}\hat{e}_x - \frac{a}{2}\hat{e}_y$, where $\frac{a}{\sqrt{3}}$ is nearest neighbor C-C distance. The unit cell is denoted by a dotted hexagon and contains two non-equivalent carbon atoms, belonging to two sub-lattices. (right) Corresponding reciprocal space is defined by $\vec{b}_1 = \frac{2\pi}{a}(\frac{\hat{e}_x}{\sqrt{3}} + \hat{e}_y)$, $\vec{b}_2 = \frac{2\pi}{a}(\frac{\hat{e}_x}{\sqrt{3}} - \hat{e}_y)$. One possible choice for Brillouin zone (BZ) is a hexagonal region of the above figure.

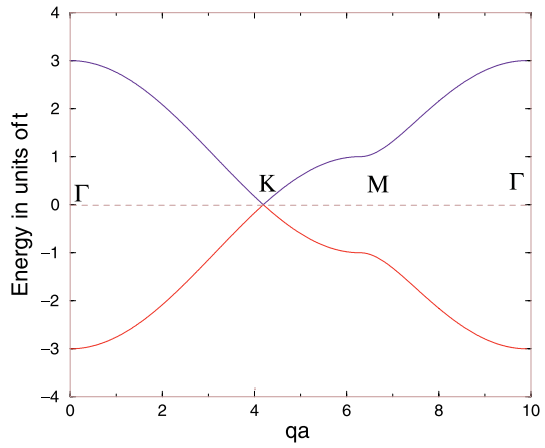

Fig. 2. π-bands of graphene along $\Gamma KM\Gamma$ loop, at tight-binding approximation. The M-point is a saddle point and gives rise to a van-Hov singularity in single-particle DOS. In this figure energy is in units of t and the horizontal axis denotes qa, with a defined in Figure 1.

For later reference, the normalized Bloch orbitals of graphene at tight-binding approximation are given by [10,11]

$$\psi^{\pm}_{\mathbf{k}}(\mathbf{r}) = \frac{1}{\sqrt{N}} \sum_{\mathbf{R}\in A} e^{i\mathbf{k}.\mathbf{R}} \phi^{\pm}_{\mathbf{k},\mathbf{R}}(\mathbf{r}) \tag{2}$$

$$\phi^{\pm}_{\mathbf{k},\mathbf{R}}(\mathbf{r}) = \frac{1}{\sqrt{2}} \left[\phi(\mathbf{r}-\mathbf{R}) \pm \frac{|f(\mathbf{k})|}{f(\mathbf{k})} e^{i\mathbf{k}.\mathbf{d}} \phi(\mathbf{r}-\mathbf{R}-\mathbf{d}) \right] \tag{3}$$

with

$$f(\mathbf{k}) = e^{i\frac{k_x a}{\sqrt{3}}} + 2e^{-i\frac{k_x a}{2\sqrt{3}}} \cos\left(\frac{k_y a}{2}\right) \tag{4}$$

where $\mathbf{R}$ runs over one of the sub-lattices of graphene and $\mathbf{R}-\mathbf{d}$ refers to carbon atom in neighboring site which lives in the other sub-lattice. Here ϕ is normalized p_z atomic orbital.

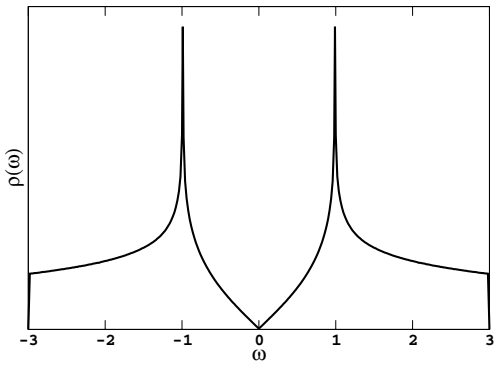

Fig. 3. The DOS corresponding to tight-binding band equation (1). The energies are in units of t. The linear behavior for small energies results form the cone-like features of the band structure near K-points and the saddle point at M-point is responsible for the cusp in DOS at $|\omega| = 1$.

The above bands after linearizing around K-points of the BZ become

$$\varepsilon_{\mathbf{k}} = \begin{cases} +\hbar v_F |\mathbf{k}| & \text{conduction band} \\ -\hbar v_F |\mathbf{k}| & \text{valence band} \end{cases} \tag{5}$$

where $\hbar v_F = \frac{\sqrt{3}}{2} ta$. The DOS associated with this linear dispersion is given by

$$\rho(\varepsilon) = \frac{1}{2\pi\hbar^2 v_F^2} |\varepsilon|.$$

So the $\rho(\varepsilon) \propto |\varepsilon|$ pseudo-gap arises form the linear features of the band structure near the K-points. It can be shown that, within DMFT, this cone-like feature remains robust against the increase in the on-site repulsion U [12]. Hence the on-site interaction does not destroy the Dirac cone picture. It only renormalizes the Fermi velocity v_F. Figures 2 and 3 depict the π bands of graphene and their corresponding DOS.

The RPA spin susceptibility

In order to calculate the contributions to total RPA susceptibility form different channels, we need the (retarded) *bare susceptibility* which is given by

$$\chi^0(\mathbf{q},\omega) = \frac{1}{N} \sum_{\mathbf{k}} \frac{f_{\mathbf{k}+\mathbf{q}} - f_{\mathbf{k}}}{\hbar\omega - (\varepsilon^c_{\mathbf{k}+\mathbf{q}} - \varepsilon^v_{\mathbf{k}}) + i0^+} \tag{6}$$

where N is the number of unit cells. At $T = 0$ the conduction band is empty and we have $f_{\mathbf{k}+\mathbf{q}} = 0$. At half filling which is the case for undoped graphene the valence band is completely filled and we have $f_{\mathbf{k}} = 1$. Therefore the bare spin susceptibility becomes (energies are in units of t, unless otherwise specified)

$$\begin{aligned} \chi^0(\mathbf{q},\omega) &= \frac{1}{N} \sum_{\mathbf{k}} \frac{-1}{\hbar\omega - (\varepsilon^c_{\mathbf{k}+\mathbf{q}} - \varepsilon^v_{\mathbf{k}}) + i0^+} \\ &= \frac{1}{N} \sum_{\mathbf{k}} \frac{1}{(\varepsilon_{\mathbf{k}+\mathbf{q}} + \varepsilon_{\mathbf{k}}) - \hbar\omega - i0^+}. \end{aligned} \tag{7}$$

Using the formula

$$\frac{1}{x-i0^+} = \mathcal{P}\frac{1}{x} + i\pi\delta(x)$$

the imaginary part of χ^0 upon can be written as

$$\begin{aligned}\mathrm{Im}\chi^0(\mathbf{q},\omega) &= \frac{\pi}{N}\sum_{\mathbf{k}}\delta\left[\hbar\omega - (\varepsilon^c_{\mathbf{k}+\mathbf{q}} - \varepsilon^v_{\mathbf{k}})\right] \\ &= \frac{A}{4\pi}\int_{BZ} d^2\mathbf{k}\;\delta\left[\hbar\omega - (\varepsilon_{\mathbf{k}+\mathbf{q}} + \varepsilon_{\mathbf{k}})\right] \qquad (8)\end{aligned}$$

where $A = \frac{\sqrt{3}a^2}{2}$ is the area of hexagonal unit cell. Using Kramers-Kronig relation, the real part of χ^0 can be obtained from the imaginary part

$$\mathrm{Re}\chi^0(\mathbf{q},\omega) = \frac{1}{\pi}\mathcal{P}\int_{-\infty}^{+\infty} d\omega' \frac{\mathrm{Im}\chi^0(\mathbf{q},\omega')}{\omega'-\omega}. \qquad (9)$$

Particle-hole continuum is a region in $\omega - \mathbf{q}$ space, where integrand of equation (8) is none-zero. Outside of this region, the denominator of the summand which gives χ^0 is none-zero and the integral becomes well-behaved and easy to perform numerically.

The contribution from the triplet particle-hole channel to the RPA spin susceptibility (particle-hole ladder summation) is given by the equation [13]

$$\chi(\mathbf{q},\omega) = \frac{\chi^0(\mathbf{q},\omega)}{1 - v(\mathbf{q})\chi^0(\mathbf{q},\omega)} \qquad (10)$$

where $v(\mathbf{q})$ is the Fourier component of potential. The short range part of the interaction is sufficient to account for the spin phenomena. Hence we use the standard Hubbard model for this tight-binding system,

$$H = -t\sum_{\langle i,j\rangle,\sigma}(c^\dagger_{i\sigma}c_{j\sigma} + c^\dagger_{j\sigma}c_{i\sigma}) + U\sum_i n_{i\uparrow}n_{i\downarrow} \qquad (11)$$

with repulsive interaction between the particles $U > 0$. For this interaction $v(\mathbf{q}) = U$ and we have

$$\chi(\mathbf{q},\omega) = \frac{\chi^0(\mathbf{q},\omega)}{1 - U\chi^0(\mathbf{q},\omega)}. \qquad (12)$$

The collective mode exists if the above RPA susceptibility has simple poles. Therefore the collective mode dispersion is given by solving the set of equations:

$$\mathrm{Im}\chi^0(\mathbf{q},\omega) = 0, \qquad \mathrm{Re}\chi^0(\mathbf{q},\omega) = \frac{1}{U}. \qquad (13)$$

One can see from equation (7) that outside the particle-hole continuum, where $\hbar\omega \neq \varepsilon_{\mathbf{k}+\mathbf{q}} + \varepsilon_{\mathbf{k}}$, we have $\mathrm{Im}\chi^0 = 0$, i.e. χ^0 is purely real. Moreover, below the particle-hole continuum $\hbar\omega < \varepsilon_{\mathbf{k}+\mathbf{q}} + \varepsilon_{\mathbf{k}}$ and thus from equation (7) one can see that $\mathrm{Re}\chi^0 = \chi^0 > 0$. This shows that below the particle-hole continuum, there could be a solution to the collective mode equations in triplet particle-hole channel.

Hence existence of a window below the particle-hole continuum provides the unique opportunity for the existence of a solution to equation (13). Therefore we need to solve equation (13) numerically. Our strategy is to fix $\mathbf{q}$ and then for a given U look for a value of omega which fulfills the collective mode criterion, equation (13). Now let us first review the neutron scattering formulation very briefly.

Neutron scattering cross section

The neutron scattering cross section is given by

$$\frac{d^2\sigma}{d\Omega dE'} = -\frac{4|\xi_{+-}|^2 r_0^2}{\pi(1-e^{-\beta\omega})}\frac{k'}{k}|F_0(\mathbf{q})|^2\mathrm{Im}\chi(\mathbf{q},\omega) \qquad (14)$$

where k, k' are incident and reflected neutron momenta, ξ_{+-} is a number of order of unity and the atomic form factor is defined by

$$F_0(\mathbf{q}) = \int d\mathbf{r}\,|\phi(\mathbf{r})|^2\,e^{i\mathbf{q}.\mathbf{r}} \qquad (15)$$

and $\phi(\mathbf{r})$ is the atomic p_z orbital.

Therefor the peak structure of neutron scattering cross section is reflected in dissipative part of the susceptibility, with an overall atomic form factor, reflecting the band nature of electrons involved in the process. The $\mathrm{Im}\chi(\mathbf{q},\omega)$ includes the effects of interaction among electrons. If we treat the effect of interaction in RPA approximation, since the life-time effects are beyond RPA, $\mathrm{Im}\chi^{RPA}$ possesses isolated sharp peaks at resonance frequencies $\omega_s(\mathbf{q})$, that is

$$\mathrm{Im}\chi^{RPA}(\mathbf{q},\omega) \approx Z(\mathbf{q})\;\delta(\hbar\omega - \hbar\omega_s(\mathbf{q})) \qquad (16)$$

which defines a dimension-less quantity $Z(\mathbf{q})$. By Kramers-Kronig relation, the above equation is equivalent to

$$\mathrm{Re}\chi^{RPA}(\mathbf{q},\omega) \approx -\frac{1}{\pi\hbar}\frac{Z(\mathbf{q})}{\omega - \omega_s(\mathbf{q})}, \qquad \omega \approx \omega_s(\mathbf{q}). \qquad (17)$$

Within the RPA, one does not need to perform any fitting to obtain $Z(\mathbf{q})$. Upon using equation (12), $Z(\mathbf{q})$ can be obtained in terms of bare susceptibility as

$$Z(\mathbf{q}) = \frac{\pi\hbar}{U^2}\left[\frac{\partial}{\partial\omega}\mathrm{Re}\chi^0(\mathbf{q},\omega)\right]^{-1}_{\omega=\omega_s(\mathbf{q})}. \qquad (18)$$

The measured intensity at an angle corresponding to momentum transfer $\mathbf{q}$, apart from overall factors, is given by

$$I(\mathbf{q}) = |F_0(\mathbf{q})|^2 Z(\mathbf{q}). \qquad (19)$$

Now let us discuss the effect of atomic form factors, which directly affects the intensity of the neutron peaks. For $2p_z$ atomic orbital, we have

$$\phi(\mathbf{r}) \sim z\;e^{-Zr/2a_0} \qquad (20)$$

where a_0 is the Bohr radius and Z is the effective nuclear charge, which for $2p$ orbitals in carbon is $\approx$1.56. Assuming

that, there is no momentum transfer along the direction perpendicular to graphene planes, the atomic form factor becomes

$$F_0(\mathbf{q}) = \frac{1}{[1+\frac{q^2a_0^2}{Z^2}]^3} \approx \frac{1}{[1+\frac{q^2a^2}{(7.8)^2}]^3}. \qquad (21)$$

Note that $a_0 \approx a/5$ where a is the lattice parameter as depicted in Figure 1. For momentum transfers much away from the center of the BZ, the atomic form factor decreases very rapidly and therefore the weight of the neutron scattering peak is suppressed by $|F_0(\mathbf{q})|^2$.

For high energy part of the collective mode branch, we will need high energy incident neutron beam. Considering the neutron kinematics, the lowest q-values which can be attained (at the lowest possible scattering angles of $\sim$2−3 degree) are relatively high, i.e. much higher than the q-vector of the first Brillouin zone. Hence, one needs to know the magnitude of the form factor at q-values from $\sim 5-12$ Å^{-1} [9] which corresponds to $qa \sim 12-29.5$. The above estimate of the atomic form factor indicates that, beyond the first BZ, the intensity of peaks is essentially zero! This makes the detection of the high energy parts a technically demanding task and the appropriate region of the BZ should be chosen carefully. Keeping this consideration in mind, after calculating the coefficient of the delta peaks of $\mathrm{Im}\chi(\mathbf{q},\omega)$ in RPA approximation, we will suggest the best regions of the BZ (Fig. 6) to be probed by neutrons.

Simplified model of cone-like bands in circular BZ

In this section we use the linearized spectrum of equation (5) as a model to evaluate χ^0 analytically [5]. In this model we assume the BZ is a circle of radius k_c which for the low-energy regime can be thought of as infinity. A single cone[1] at the center of the circular BZ is just an assumption. Note that in real graphite there are two such a cones. Such a simplified model seems to capture the essential low-energy physics of band structure (1). The linear spectrum of equation (5) holds over a fairly large range of energies (up to $\epsilon \sim 0.5t \sim 1$ eV) which can be seen qualitatively from the density of states (Fig. 3). Such a model will be relevant to

- Wave vectors near K-point, of course with modified parameters such as Fermi velocity v_F, etc.
- Wave vectors near Γ-point. The analytical knowledge gained about the small-q behavior of the dispersion of spin collective mode will enable us to see the qualitative difference between the case of an isolated graphene sheet and a real graphite in which the long-range (small-q) tail of the interaction becomes essential. We will include these effect analytically and will see that at Γ-point which is susceptible for instability, the collective mode still survives.

[1] A covariant formulation in terms of Dirac spinors, should take care of 2 cones, 2 chiralities, and 2 spin degrees of freedom, which requires a $2^3 = 8$ component formalism.

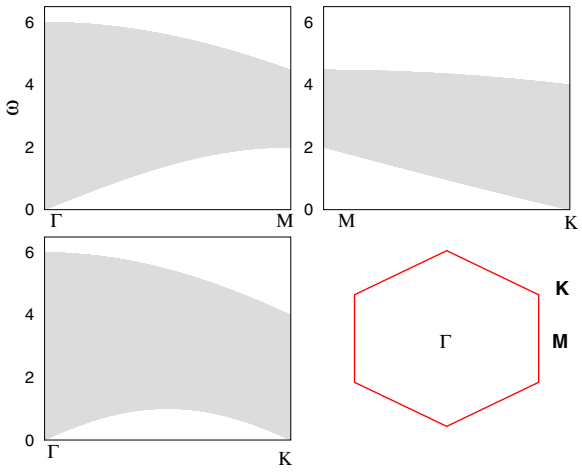

Fig. 4. Particle-hole continuum of graphite. Horizontal axis is center of mass momentum of particle-hole pair and vertical axis is the particle-hole energy. Gray region is the particle-hole continuum, corresponding to the spectrum given by equation (1). The energies are in units of t. This is obtained for a fixed $\mathbf{q}$, by finding the maxima and minima of the particle-hole energy $\varepsilon_{\mathbf{q}+\mathbf{k}} + \varepsilon_{\mathbf{k}}$ for random walker $\mathbf{k}$ walking in Brillouin zone.

Moreover, it will teach us a mechanism by which the system exhibits certain effective 1D characters. It turns out that the very same mechanism is responsible for the existence of the spin collective mode over a large fraction of BZ area.

Starting with equation (8)

$$\mathrm{Im}\chi^0(\mathbf{q},\omega) = \frac{A}{4\pi}\int_{|\mathbf{k}|<k_c} \delta\left[\hbar\omega - \hbar v_F(|\mathbf{k}+\mathbf{q}|+|\mathbf{k}|)\right] = \frac{A}{4\pi\hbar v_F}\int \frac{ds}{|\nabla_k f_{\mathbf{q}}(\mathbf{k})|_{f_{\mathbf{q}}(\mathbf{k})=z}} \qquad (22)$$

where

$$f_{\mathbf{q}}(\mathbf{k}) = |\mathbf{k}-\mathbf{q}| + |\mathbf{k}|, \qquad z = \frac{\omega}{v_F}$$

and ds is the length element on $f_{\mathbf{q}}(\mathbf{k}) = z$. The equation $f_{\mathbf{q}}(\mathbf{k}) = |\mathbf{k}-\mathbf{q}|+|\mathbf{k}| = z$ defines and ellipse with principal axis equal to $\frac{q}{2}$ and half canonic distance equal to $\frac{z}{2} = \frac{\omega}{2v_F}$. Therefor $\mathrm{Im}\chi^0$ is none zero if and only if

$$z > q \Rightarrow \omega > v_F q \qquad \text{particle-hole continuum.} \qquad (23)$$

This result should be compared with Figure 4 around K-point and Γ-point.

Assuming that ϕ is the angle between $\mathbf{q}$ and $\mathbf{k}$ and $k = |\mathbf{k}|$, the equation of ellipse becomes

$$k = \frac{z^2 - q^2}{2(z - q\cos\phi)} \qquad (24)$$

which gives

$$\begin{aligned} dk &= -\frac{q(z^2-q^2)\sin\phi}{2(z-q\cos\phi)^2}d\phi \\ ds &= \sqrt{k^2d\phi^2+dk^2} \\ &= \frac{z^2-q^2}{2(z-q\cos\phi)^2}\sqrt{z^2+q^2-2zq\cos\phi} \\ |\nabla_k f_{\mathbf{q}}(\mathbf{k})| &= \frac{2(z-q\cos\phi)}{\sqrt{z^2+q^2-2zq\cos\phi}}. \end{aligned} \tag{25}$$

Putting every thing together we obtain

$$\begin{aligned} \mathrm{Im}\chi^0(\mathbf{q},\omega) &= \frac{z^2-q^2}{16\pi\hbar v_F}\int\frac{z^2+q^2-2zq\cos\phi}{(z-q\cos\phi)^3}\,d\phi \\ &= \frac{1}{16\hbar v_F}\frac{2z^2-q^2}{\sqrt{z^2-q^2}} \\ &= \frac{\sqrt{3}a^2}{16\hbar v_F^2}\frac{\omega^2-\frac{1}{2}v_F^2q^2}{\sqrt{\omega^2-v_F^2q^2}}, \quad qv_F<\omega<(2k_c+q)v_F \end{aligned} \tag{26}$$

where in last step we have used $A=\frac{\sqrt{3}}{2}a^2$ to restore the lattice parameter a. If we take the limit $\omega\to v_Fq$, this equation reduces to the edge propagator given by equation (2) of reference [14]. To obtain the real part, we use Kramers and Kronig relation, equation(9); along with change of variables $\omega'=qv_F\coth\eta$, $\coth\eta_0=1+\frac{2k_c}{q}$. To leading order in $\frac{2k_c}{q}$ we have

$$\begin{aligned} \mathrm{Re}\chi^0(\mathbf{q},\omega) &= \frac{\sqrt{3}a^2}{32\hbar\pi v_F^2}\int_{qv_F}^{2k_cv_F}\frac{d\omega'}{\omega'-\omega}\frac{2\omega^2-v_F^2q^2}{\sqrt{\omega^2-v_F^2q^2}} \\ &= -\frac{\sqrt{3}a^2q^2}{32\pi\hbar}\int_{\eta_0}^{\infty}d\eta\frac{2\coth^2\eta-1}{\sinh\eta(\omega-qv_F\coth\eta)} \\ &= -\frac{\sqrt{3}a^2}{16\pi\hbar v_F^2}\Bigg[\omega\log\left(\frac{4k_c}{q}\right)-qv_F\left(\frac{2k_c}{q}+1\right) \\ &+\frac{q^2v_F^2-2\omega^2}{\sqrt{q^2v_F^2-\omega^2}}\left(\arctan\sqrt{\frac{qv_F-\omega}{qv_F+\omega}}-\frac{\pi}{2}\right)\Bigg]+\mathcal{O}\left(\frac{q}{k_c}\right) \\ &= \frac{\sqrt{3}k_ca^2}{8\pi\hbar v_F}+\frac{\sqrt{3}a^2}{16\pi\hbar v_F^2}\frac{2\omega^2-q^2v_F^2}{\sqrt{q^2v_F^2-\omega^2}}\arctan\sqrt{\frac{qv_F+\omega}{qv_F-\omega}} \\ &+\mathcal{O}\left(\log\frac{k_c}{q}\right), \qquad qv_F>\omega. \end{aligned} \tag{27}$$

Now going back to equations (13) we see that in region $qv_F>\omega$ where the above formula for $\mathrm{Re}\chi^0(\mathbf{q},\omega)$ is valid, the imaginary part is identically zero. So the dispersion of collective mode is the solution to equation

$$\frac{1}{U}=\frac{\sqrt{3}k_ca^2}{8\pi\hbar v_F}+\frac{\sqrt{3}a^2}{16\pi\hbar v_F^2}\frac{2\omega^2-q^2v_F^2}{\sqrt{q^2v_F^2-\omega^2}}\arctan\sqrt{\frac{qv_F+\omega}{qv_F-\omega}}. \tag{28}$$

Near the particle-hole boundary the RHS of the above equation can be expanded to obtain (note that $\hbar v_F=ta\sqrt{3}/2$)

$$\frac{1}{U}=\frac{k_ca}{4\pi t}+\frac{\sqrt{3}a^2q^{3/2}}{32\hbar\sqrt{2v_F}\sqrt{qv_F-\omega}}+\mathcal{O}(qv_F-\omega)^{1/2}. \tag{29}$$

The above equation has a solution, passing through the origin for any value of $U<U_1=\frac{4\pi t}{k_ca}$. To get some idea about the value of U_1, let us choose k_c in such a way that the area of our circular BZ is equal to the area of hexagonal BZ of the original problem, that is

$$\pi k_c^2=\frac{8\pi^2}{\sqrt{3}\,a^2}\Rightarrow k_ca=2\left(\frac{2\pi}{\sqrt{3}}\right)^{1/2}\approx 3.81$$

which gives $U_1=\left(2\pi\sqrt{3}\right)^{1/2}t\approx 3.30t$. Hence to leading order in qa the dispersion of the spin-1 collective mode near the Γ-point becomes

$$\omega_s(\mathbf{q})=v_Fq(1-\alpha^2a^2q^2)=v_Fq-\omega_B(q), \tag{30}$$

as $\omega\to v_Fq\to 0$ where

$$\alpha=\frac{1}{8\sqrt{6}}\frac{UU_1}{t(U_1-U)}.$$

Note that equation (30) makes sense only if $\left|\alpha^2a^2q^2\right|\ll 1$. In particular the smallness of α implies that U must be below U_1 and far enough from it. In fact, numerical calculations with full band structure shows that for $U>U_c\approx 2.23\ t$, an instability emerges around the Γ-point (see Fig. 5). Since the linear model is relevant to Γ-point (and also the K-point, but with renormalized v_F), the requirement of $U<U_1$, warns us about an instability. However, since the real graphite is stable, the normalized value of interaction must be less than $2.23\ t$ and we are not worried about it. Here $\hbar\omega_B$ is the binding energy of particle-hole pairs with center of mass momentum equal to $\mathbf{q}$. The repulsive interaction U among particles becomes attractive for particle-hole pairs in triplet spin state and binds them together to form a bound state with binding energy $\hbar\omega_B$. To see why there exists a bound state for arbitrarily small attraction U, note that, right above the particle-hole continuum and very close to the continuum boundary, $\mathrm{Im}\chi^0$ can be written as

$$\mathrm{Im}\chi^0(\mathbf{q},\omega)=\frac{\sqrt{3}a^2}{32\hbar\sqrt{2v_F}}\frac{q^{3/2}}{\sqrt{\omega-qv_F}} \tag{31}$$

with a square root divergence at the lower edge of the particle-hole continuum in $\omega-\mathbf{q}$ space. This expression has the same form as the one dimensional density of states (with energy measured from $\hbar qv_F$). Note that, in fact, $\mathrm{Im}\chi^0(\mathbf{q},\omega)=\pi\rho_{\mathbf{q}}(\omega)$, where $\rho_{\mathbf{q}}(\omega)$ is the free particle-hole DOS for a fixed center of mass momentum q. That is, the particle-hole pairs have a phase space for scattering which is effectively one dimensional. Thus we have a bound state of particle-hole pairs in spin-triplet channel for arbitrarily small interaction U. However, we also have a pre factor $q^{3/2}$ which scales the density of states. This together with the square root divergence of the density of states at the bottom of the particle-hole continuum gives us a bound state for every $\mathbf{q}$ as $q\to 0$, with the binding energy vanishing like $\sim q^3$ as shown above. Equation (31) shows that region responsible for the formation of spin-1 zero sound (SZS) near the Γ and K-points, is mainly

near the bottom of the particle-hole continuum. In fact for center of mass momenta close to Γ, K-points, there will be a one dimensional manifold on which the particle-hole energy has its minimum and this one-dimensional manifold of minima is responsible for square root divergence in particle-hole DOS. The M-point has a similar property. These explains why for center of mass momentum corresponding to M-point too, the spin-1 collective mode is there for arbitrarily small interaction U.

Neutron resonance peaks for the cone model

Plugging equations (27) and (30) into the above equation, it is straightforward to show that near the Γ and K-point the peak intensity behaves like

$$Z(\mathbf{q}) = \frac{3\pi^4}{4}\frac{Ut^2}{(U_1-U)^3}\left(\frac{q}{k_c}\right)^3 \times \left\{1 - 15\pi^2\frac{U^2}{(U_1-U)^2}\left(\frac{q}{k_c}\right)^2 + \mathcal{O}\left(\frac{q}{k_c}\right)^3\right\}. \quad (32)$$

This equation shows that for a graphene layer the resonance peak residue, $Z(\mathbf{q})$ vanishes as $\sim q^3$, where $\mathbf{q}$ is measured from Γ or K-points of the BZ. The cross section for momentum transfers near Γ and K are very small. Vanishingly small $Z(\mathbf{q})$ according to Appendix A, means spatially large wave-function which can not be excited by neutrons with a typical de-Broglie wave-length of $\sim$1 Å.

Due to the presence of the other graphene layer and screening arising from the interlayer hopping among the layers, the power law $Z(\mathbf{q}) \sim q^3$ may change in real 3D graphite. In next subsection, we will discuss the effect of semi-metallic screening, which amounts to taking into account the long range tail of the interaction among the electrons.

Effect of long-ranged part of the interaction

Having established the existence of a gapless spin-1 collective mode branch within Hubbard model and the RPA approximation, we will discuss whether the semi-metallic screened interaction of 3D stacked layers will affect our result. In tight binding situation like ours, the spin physics is mostly captured by the short range part of the repulsion among the electrons. So we do not expect a drastic change in the behavior of spin collective mode, if we correct the interaction, by including long range tails, i.e. modifications near $\mathbf{q} = 0$.

Interaction, including interlayer scattering between layers separated by distance d is given by [14,15]

$$\tilde{v}(\omega, q) = \frac{2\pi e^2}{\epsilon_0 q}\frac{\sinh(qd)}{\sqrt{[\cosh(qd) + \frac{2\pi e^2}{\epsilon_0 q}\sinh(qd)\chi_0(\omega,q)]^2 - 1}}.$$

Let us assume that the asymptotic behavior of $\tilde{v}(\omega, q)$ of the above equation at long wave-lengths is $q^{-\nu}$, where we will determine the exponent ν self-consistently. From right hand side of equation (29), we have

$$\mathrm{Re}\chi(\mathbf{q}, \omega) = a + \frac{b\ q^\eta}{\sqrt{q-\omega}} \quad (33)$$

where $\eta = 3/2$, and we have assumed $v_F = 1$. Moreover, inspired by our previous results, we assume the following ansatz for the dispersion of the collective mode in presence of a long range interaction $\tilde{v}(\omega, q)$:

$$\omega_s(\mathbf{q}) = q - cq^\beta \quad (34)$$

where a, b, c in above equations are numerical constants

Using the Kramers-Kronig relation, the collective mode equation becomes

$$\begin{aligned} q^\nu \sim \frac{1}{\tilde{v}(q)} = \mathrm{Re}\chi^0(\mathbf{q}, \omega_s(\mathbf{q})) &\sim \int \frac{d\omega'}{\omega' - \omega_s(\mathbf{q})}\frac{q^\eta}{\sqrt{\omega' - q}} \\ &= q^\eta \int \frac{d\sqrt{\omega' - q}}{\omega' - \omega_s(\mathbf{q})} = q^\eta \int \frac{du}{u^2 + q - \omega_s(\mathbf{q})} \\ &= q^\eta \int \frac{du}{u^2 + cq^\beta} \sim q^{\eta - \beta/2} \end{aligned}$$

that gives

$$\beta = 2(\eta - \nu). \quad (35)$$

This equation is important in that, it determines the qualitative difference between the dispersion of the collective mode in graphene and graphite. In our case $\eta = 3/2$. The graphene is characterized by $\nu = 0$, or equivalently $\beta = 3$ which is nothing, but equation (30). Since $\eta = 3/2$, in addition to equation (35) we need another equation to determine these exponents self-consistently. This equation will be provided by Taylor expansion of $\tilde{v}(\omega, q)$.

Substituting the ansatz (34) in equation (33), one can see that $\mathrm{Re}\chi \sim a + b'q^{\eta - \beta/2} \sim a + b'q^{\nu/2}$, where in the last step we have used equation (35). Using the above expression for $\mathrm{Re}\chi(\omega, q)$ in RHS of defining expression of $\tilde{v}(\omega, q)$, to leading order we obtain:

$$\tilde{v}(\omega, q) \sim \text{const.} = U' \Rightarrow \nu = 0. \quad (36)$$

This equation tells us that as far as the existence of a solution of type (34) in spin channel is concerned, the long ranged part of the Coulomb interaction in graphite is only going to renormalize the Hubbard U of a single graphene layer. Therefore even in presence of a long range interaction, we have $\beta = 3/2$, and the qualitative picture resulting from the simple Hubbard model for a single graphene layer is not going to change. At this level, the only quantitative difference between a single layer of graphene and stacks of graphene in real graphite, with their long ranged Coulomb interaction included, would be in coefficient c of equation (34).

Let us go back to equation (35) to discuss the importance of the prefactor $q^\eta = q^{3/2}$ in DOS of particle-hole pairs in graphite. The case of strictly one-dimensional problem corresponds to $\eta = 0$. So a none zero η is a peculiar feature of our particular problem which should be

taken into account in putting 1D-like features in a formal basis in a bosonization approach. It can be seen from equation (35) that for the case of a real 1D problem $\beta = -2\nu$. Since in semi-metallic and insulator case $\nu > 0$, then the exponent β becomes negative and hence the expansion (34) makes no sense. Therefor a bare 1D DOS (square root divergence) is not sufficient to bound electron-hole pairs together to form spin-1 zero sound (SZS). To conclude, both square root and $q^{3/2}$ pre-factor are essential to manage a gapless spin-1 collective mode in graphite.

One can also use a similar asymptotic analysis to reproduce the dependence of $Z(\mathbf{q})$ on q. Differentiating Kramers-Kronig relation, equation (9) with respect to ω and using (34) gives

$$\left.\frac{\partial}{\partial\omega}\chi^0(\mathbf{q},\omega)\right|_{\omega=\omega_s(\mathbf{q})} \sim q^\eta \int \frac{d\sqrt{\omega'-q}}{(\omega'-\omega_s(\mathbf{q}))^2} \sim q^\eta \int \frac{du}{(u^2+q-\omega_s(\mathbf{q}))^2} = q^\eta \int \frac{du}{(u^2+cq^\beta)^2} \sim q^{\eta-3\beta/2}.$$

Using equations (18) and (35) we obtain

$$Z(\mathbf{q}) \sim q^{2\eta-3\nu}. \tag{37}$$

The case of a single layer of graphene, and real graphite correspond to $\eta = 3/2$ and $\nu = 0$, with just different proportionality constants which gives rise to q^3 dependence in agreement with equation (32). The above analysis reveals that, following properties conspire to manage a spin-1 collective mode in a cone model for graphite:

1. Dirac cone spectrum, i.e. a pseudo-gap of the form $g(\epsilon) = |\epsilon|$ that allows for a window below the particle-hole continuum and to produce a semi-metallic screening $\tilde{v}(q) \sim q^{-1/2}$ for 3D stack of graphite.
2. Square root divergence of the DOS of free particle-holes at the edge of particle-hole continuum, accompanied by $q^{3/2}$ factor that comes form two dimensionality of the original problem.

Numerical calculation of the weight of neutron scattering peaks

So far our cone model that was appropriate to describe the small-q behavior of the collective mode was especially suitable to address the physics near the Γ-point (and also K-point, with renormalized parameters), e.g. the question of modifications arising form inclusion of the long-range tail of interaction which arises form the stacks of graphene layers in real 3D graphite. But for the neutron scattering experiments, we need to repeat the calculations in entire BZ. To find the resonance frequencies $\omega_s(\mathbf{q})$ in entire BZ, we have to numerically solve for equation (13). In order to do so we have to perform the summation (7) or equivalently

$$\mathrm{Re}\chi^0(\mathbf{q},\omega) = \frac{\sqrt{3}\ a^2}{8\pi^2}\int_{BZ} \frac{d^2\mathbf{k}}{(\varepsilon_{\mathbf{k}+\mathbf{q}}+\varepsilon_{\mathbf{k}})-\hbar\omega} \tag{38}$$

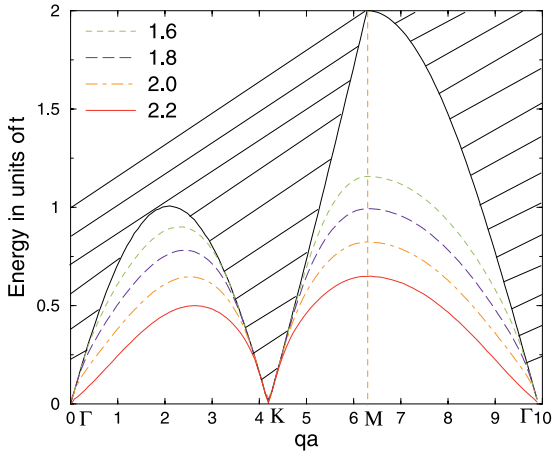

Fig. 5. The spin-1 collective mode for different values of U. Note the emergence of instability at Γ-point at $U \approx 2.2$. Also note the asymptotic behavior of the dispersion of the spin-1 collective mode near Γ and K-points. According to analysis of the single cone model, the collective mode dispersion near these points asymptotically approaches the continuum boundary. At M-point the resonance energy is at $\sim 0.83 \times t \approx 2.0$ eV and is well isolated from the boundary of p-h continuum. Lower energy regions are toward Γ and K-points. Toward Γ-point binding energies are larger and better for neutron scattering as discussed in the text.

where $A = \frac{\sqrt{3}}{2}a^2$ is the area of units cell. We know form our analytical solutions that, below a certain value of U, the solution to collective mode equation (13) lies below the particle-hole continuum and asymptotically approaches the lower boundary of continuum at K and Γ-point. Hence the denominator of the integrand in the above equation inside the region in which we must look for the solutions $\omega_s(\mathbf{q})$ is none zero. Therefore with full band dispersion of equation (1), such integrals can be numerically performed, without any problems. However, numerically it becomes more and more difficult to get the square root divergences as we go closer and closer to K-point. This is because of the pre-factor $q^{3/2}$ in equation (31).

Figure 5 shows the numerical evaluation of the dispersion of spin-1 collective mode for different values of U. As can be seen in Figure 5, near K-point the collective mode pole is very close to the continuum boundary. One can fit a dispersion of type (30) near Γ and K-points, but the coefficients will be different from that given by equation (30). Since near the K-point the binding energies are very small, the particle-hole pairs are bound loosely and the spatial extent of their wave-function is large which makes it difficult to excite them by neutrons with typical wave-length $\lambda \sim$ Å. Therefore we suggest the neutron scattering experiments, NOT to focus around the K-points. For the same reason the region very close to Γ-point should be avoided.

Note that in Figure 5, at M-point, there is a collective mode pole for any value of U. In fact at this point, the DOS of free particle-hole pairs diverges as $\sim 1/\sqrt{\omega - 2t}$, where $2t$ corresponds to bottom of the particle-hole continuum at M. Bindings at M-point and its neighborhood, especially toward Γ, and also the point mid-way

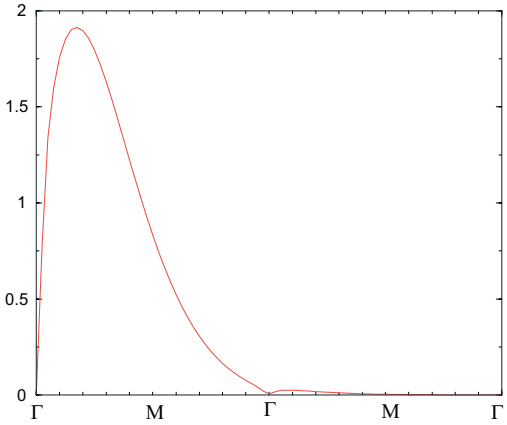

Fig. 6. Plot of $I(\mathbf{q}) = |F_0(\mathbf{q})|^2 Z(\mathbf{q})$ as a function of momentum transfer along ΓM direction. The $\Gamma\Gamma$ distance is ≈ 3 Å^{-1}. Because of the effective nuclear charge $Z = 1.56$ for $2p_z$ orbitals, the form factor decays very quickly, so that beyond the first BZ it is almost zero. This figure suggests that the M point is not suitable for neutron scattering. Since momentum transfers in 2nd $-$ 4th BZ ($5 - 12$ Å^{-1}) are involved at which peak intensity is almost zero (see the discussion following Eq. (21)).

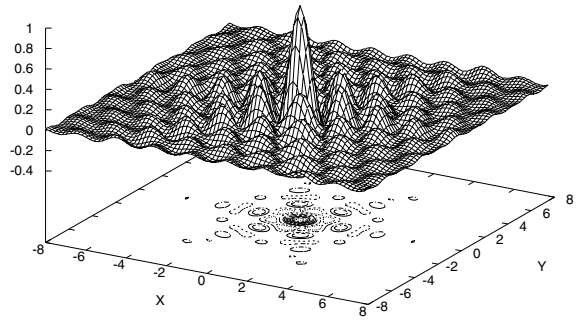

Fig. 7. The approximate bound state wave-function within the RPA approximation. The center of mass momentum $\mathbf{q}$ is at $0.2\ \Gamma M \approx 0.3$ Å^{-1}. Unit of length is the lattice parameter $a \approx 2.46$ Å. Contours corresponding to $|\psi_{\mathbf{q}}(\mathbf{r})| > 0.1$ have been plotted in the base. Note a very soft anisotropic pattern of contours. The normalization of the wave-function is such that $\psi_{\mathbf{q}}(0) = 1$. This figure explicitly demonstrates why at low energies we have a collective mode. We expect $\sim$0.5 eV neutrons to be able to excite such a bound state.

between ΓK and region toward Γ are strong enough to give rise to a particle-hole pairs, with small enough wave functions that can be excited by thermal hot and epithermal neutrons. At M-point, the resonance energy is $\sim$2 eV, but since at these energies momentum transfers beyond the first BZ are involved, the atomic form factor strongly reduces the intensity of neutron peaks. This makes neutron scattering at M-point a challenge. Therefore despite the large binding energy, this point is not a good candidate to focus the neutron scattering experiments. We will give a qualitative picture of wave-function in the following. Note the emergence of an instability at Γ-point near $U_c \approx 2.2t$. Indeed at the level of a Hartree-Fock mean field one finds a transition to FM phase at

$$U_c = \frac{1}{\chi^0(\mathbf{q}=0,\omega=0)} \approx 2.231t.$$

However, real graphite for which $U \sim 4t - 5t$ is stable. So the value of $U_c = 2.23t$ should be an artifact of RPA approximation, and one expects by going beyond the RPA, to push U_c above the $2.23t$ or equivalently to obtain an screened value of U below $2.23t$ [16]. Assuming that the renormalized value of U is less than $2.23t$, we will perform the rest of calculations for $U = 2t \sim 5$ eV.

Once we find the location of resonance frequencies $\omega_s(\mathbf{q})$, the next step is to calculate $Z(\mathbf{q})$. The trick is to use the formula (18), but with $\left[\frac{\partial}{\partial\omega}\mathrm{Re}\chi^0(\mathbf{q},\omega)\right]_{\omega=\omega_s(\mathbf{q})}$ given by direct differentiation of equation (38), that is

$$Z(\mathbf{q}) = \frac{\pi}{U^2}\left(\sum_{\mathbf{k}} \frac{1}{[\varepsilon_{\mathbf{k}+\mathbf{q}} + \varepsilon_{\mathbf{k}} - \hbar\omega_s(\mathbf{q})]^2}\right)^{-1} \quad (39)$$

$$= \frac{8\pi^3}{\sqrt{3}\ U^2 a^2}\left(\int \frac{d^2\mathbf{k}}{[\varepsilon_{\mathbf{k}+\mathbf{q}} + \varepsilon_{\mathbf{k}} - \hbar\omega_s(\mathbf{q})]^2}\right)^{-1}. \quad (40)$$

Then using equations (19) and (21) the weight of neutron scattering peaks $I(\mathbf{q})$, can be calculated, which is depicted in Figure 6. The maximum value of the $I(\mathbf{q})$ for $\mathbf{q}$ along ΓM, lies between $\sim 0.1\ \Gamma\Gamma = 0.2\ \Gamma M \approx 0.3$ Å^{-1} and $\sim 0.2\ \Gamma\Gamma = 0.4\ \Gamma M \approx 0.6$ Å^{-1}. At these wave vectors the energies of neutrons lie between $\sim$0.5 eV and $\sim$1 eV which are much easier for neutron scattering than $\sim$2 eV at the M-point. Profile of the peak intensity along ΓK is shown in Figure 6. Therefore according to this calculation, the best chance of detecting spin-1 collective mode, is at the points between ΓM and ΓK which are closer to Γ, than K or M.

Note that for these points, $I(\mathbf{q})$ becomes of the order of unity and the binding energy are typically $\hbar\omega_B \gtrsim 1$ eV. For larger values of $I(\mathbf{q})$ it is easier to excite the triplet exciton. Equation (48) of Appendix A, explicitly shows the relationship between spatial extent of the excitonic wave-function and $Z(\mathbf{q})$. The small binding energies correspond to loosely bound particle-hole pairs and hence large wave-functions, which is according to (48) synonymous to small peak intensities. Intuitively speaking, it becomes harder to excite larger objects by neutrons of wave-length $\lambda \sim$ Å.

Very close to Γ-point, according to (32) $I(\mathbf{q}) \approx Z(\mathbf{q}) \sim q^3$ that corresponds to very large wave-functions. However as one expects form the qualitative behavior of binding energies (Fig. 5) and also the qualitative behavior of $I(\mathbf{q})$ (Fig. 6), as q deviates a bit away form Γ-point, the wave-function becomes of the order of a few lattice constants and hence visible by neutrons (Fig. 7).

In Figures 7 and 8 the contours show the region in which $|\psi_{\mathbf{q}}(\mathbf{r})| > 0.1$ which roughly corresponds to the spatial extent of the bound-state wave-function. They respectively correspond to $\mathbf{q} = 0.2\times\overrightarrow{\Gamma M}$ and $\mathbf{q} = \overrightarrow{\Gamma M}$. The normalization of the wave-function is such that $\psi_{\mathbf{q}}(\mathbf{r}=0) = 1$. As can be seen form comparison of two figures, the spatial extent of the bound-state wave function for center of mass momentum corresponding to M-point, is of the order of two unit cells with highly anisotropic nature.

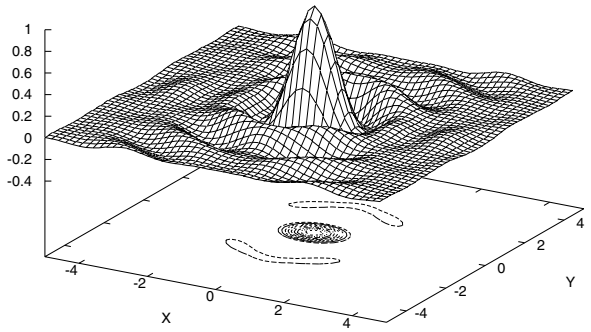

Fig. 8. The approximate bound state wave-function within the RPA approximation. The center of mass momentum $\mathbf{q}$ is at the M-point. Unit of length is the lattice parameter $a \approx 2.46$ Å. Contours corresponding to $|\psi_{\mathbf{q}}(\mathbf{r})| > 0.1$ have been plotted in the base. Note the anisotropic pattern of contours. The normalization of the wave-function is such that $\psi_{\mathbf{q}}(0) = 1$. At this point the spatial extent of the bound state wave-function is not so large and it can be identified with triplet excitons. This state can not be excited so easily. Since it requires momentum transfers beyond the first BZ, at which atomic form factors wash out the neutron peak.

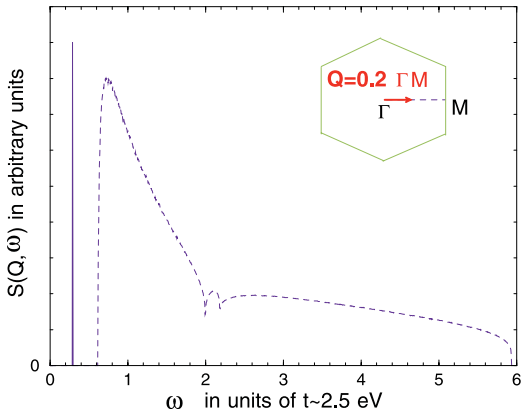

Fig. 9. $\mathrm{Im}\chi^{RPA}(\omega)$ as a function of ω at $\mathbf{Q} = 0.2\Gamma M \approx 0.3$ Å^{-1}. Note that ω in this figure is in units of t. The particle-hole continuum is clearly seen in this figure (dashed line). Below the continuum at $\omega_s(\mathbf{Q}) \approx 0.30\ t \approx 0.7$ eV a very sharp peak in $\mathrm{Im}\chi^{RPA}$ shows up (solid line).

Discussions

Now let us discuss the effect of σ bands. The σ bands have their minima centered around the Γ-point. If we fit a quadratic dispersion to LDA data, we find that the inclusion of excitation form valence π band to σ band do not modify the collective mode qualitatively. The height of the window below the particle-hole continuum of Figure 4 along the ΓK is not very high. Therefore the excitations to σ do not shrink the window along ΓK. However around M-point, at which the height of window is $2t$, the inclusion of excitations to σ band, reduce the height by maximum amount of $\sim 0.5t$ at the M-point. But as can be seen from Figure 5, this does not open a decay channel for the collective mode branch corresponding to normalized $U \sim 2t$.

Recently, Peres and coworkers have criticized our method of calculating the RPA spin susceptibility [19]. We have clarified the issue in detail [20].

In conclusion, we have evaluated the spin susceptibility of a graphene layer in RPA approximation for a short range interaction. We obtained a magnetic (spin-1) collective mode branch in non magnetic phase of graphite which exists in entire BZ with a very wide energy range form zero at Γ and K to ∼2 eV near the M-point. This branch is below the particle-hole continuum and is protected from Landau damping. Therefore it might provide a mechanism for transport of spin-only currents, over a wide energy range. We showed that the long range tail of the Coulomb interaction in real graphite (3D stacks of graphene) does not destroy the conclusions drawn from the Hubbard interaction. We also presented the calculation of the weight of the neutron peaks. The most appropriate region of the BZ to focus the neutron scattering experiments is region in between Γ and M and region mid-way between Γ and K-points (closer to Γ than M or K). Hot or epithermal neutrons ($0.1 - 1.0$ eV) are more appropriate for this region of momentum transfers. The dynamical form factor for a typical momentum transfer in the above region is schematically plotted in Figure 9. At the above mentioned regions, in one hand one does not require very high energy neutrons; on the other hand, the binding is strong enough to lead to small enough wave-functions which can be excited with hot or epithermal neutrons.

S.A. Jafari appreciates the Third World Academy of Sciences (TWAS) for financial support under TWAS fellowship for post-doctoral research and advanced training and the Institute of Mathematical Sciences (IMSc), Chennai, India, for hospitality. We thank Dr. Amir Murani for encouraging discussions and correspondence on the possibility of study of spin-1 collective modes in graphite by neutron scattering.

Appendix A: Excitonic wave-function approach to spin collective mode

One can see more closely the relation between the $Z(\mathbf{q})$ and the binding energies and real space profile of the wave-function as follows. At the RPA approximation, the eigenvector of the exciton state with spin S can be written as a linear combination of all the product eigenvectors of free charge carriers created in the crystal [17,18]

$$|\mathbf{q}, S\rangle^{ex} = \sum_{\mathbf{k}'} g_{\mathbf{q}}(\mathbf{k}')\ |\mathbf{k}' + \mathbf{q}, -\mathbf{k}'; S\rangle \qquad (41)$$

where we have used the free electron-hole basis $|\mathbf{k} + \mathbf{q}, -\mathbf{k}; S\rangle$ to expand the exciton wave-function. The triplet one which is relevant to our case is given by

$$|\mathbf{k}+\mathbf{q}, -\mathbf{k}; 1\rangle = \frac{1}{\sqrt{3}}\left(c^{c\dagger}_{\mathbf{k}+\mathbf{q}\uparrow} d^{v\dagger}_{-\mathbf{k}\uparrow} + c^{c\dagger}_{\mathbf{k}+\mathbf{q}\downarrow} d^{v\dagger}_{-\mathbf{k}\downarrow}\right)|0\rangle + \frac{1}{\sqrt{6}}\left(c^{c\dagger}_{\mathbf{k}+\mathbf{q}\uparrow} d^{v\dagger}_{-\mathbf{k}\downarrow} + c^{c\dagger}_{\mathbf{k}+\mathbf{q}\downarrow} d^{v\dagger}_{-\mathbf{k}\uparrow}\right)|0\rangle$$

where $d^{v\dagger}_{-\mathbf{k}-\sigma} \equiv c^{v}_{\mathbf{k}\sigma}$ creates a hole with spin projection $-\sigma$ and momentum $-\mathbf{k}$. The exciton eigenvalue problem in free p-h basis becomes [17]

$$[E^c(\mathbf{k}+\mathbf{q}) - E^v(\mathbf{k}) - W_{\mathbf{q}}]\, g_{\mathbf{q}}(\mathbf{k}) - U \sum_{\mathbf{k}'} g_{\mathbf{q}}(\mathbf{k}') = 0. \quad (42)$$

Here $E^c(\mathbf{k}+\mathbf{q})$ and $E^v(\mathbf{k})$ are total energies of single particle in conduction and valence band including their interaction energy with the other electrons of the band. The interaction between different pairs is included in constant kernel $-U$ [18]. In triplet channel the kernel becomes a direct Coulomb term and moreover it is attractive.

The RPA approximation amounts to ignore the self-energy effects and write (i.e. solving a two-body problem)

$$E^c(\mathbf{k}+\mathbf{q}) \to \varepsilon^c_{\mathbf{k}+\mathbf{q}/2} = \varepsilon_{\mathbf{k}+\mathbf{q}/2} \quad (43)$$

$$E^v(\mathbf{k}) \to \varepsilon^v_{\mathbf{k}-\mathbf{q}/2} = -\varepsilon_{\mathbf{k}-\mathbf{q}/2}. \quad (44)$$

Note that wave-vectors are such that the wave-equation becomes manifestly time reversal invariant ($\mathbf{k} \to -\mathbf{k}$), as can be seen from the wave-equation below

$$\left[\varepsilon_{\mathbf{k}+\mathbf{q}/2} + \varepsilon_{\mathbf{k}-\mathbf{q}/2} - \hbar\omega_s(\mathbf{q})\right] g_{\mathbf{q}}(\mathbf{k}) - U \sum_{\mathbf{k}'} g_{\mathbf{q}}(\mathbf{k}') = 0.$$

Let $\sum_{\mathbf{k}'} g_{\mathbf{q}}(\mathbf{k}') = C$, solve for $g_{\mathbf{q}}(\mathbf{k})$ and sum over $\mathbf{k}$ to obtain the self-consistency equation

$$C = \sum_{\mathbf{k}} \frac{UC}{\varepsilon_{\mathbf{k}+\mathbf{q}/2} + \varepsilon_{\mathbf{k}-\mathbf{q}/2} - \hbar\omega_s(\mathbf{q})} \quad (45)$$

which is exactly equivalent to the RPA approximation, equation (13). The wave-function of the single particle-hole pair can be approximated by Fourier transform[2] of $g_{\mathbf{q}}(\mathbf{k})$. Thus we have

$$\psi_{\mathbf{q}}(\mathbf{r}) = \frac{1}{N} \sum_{\mathbf{k}} \frac{\exp(i\mathbf{k}\cdot\mathbf{r})}{\varepsilon_{\mathbf{k}+\mathbf{q}/2} + \varepsilon_{\mathbf{k}-\mathbf{q}/2} - \hbar\omega_s(\mathbf{q})} \quad (46)$$

$$= \frac{A}{4\pi^2} \int d^2\mathbf{k} \frac{\exp(i\mathbf{k}\cdot\mathbf{r})}{\varepsilon_{\mathbf{k}+\mathbf{q}/2} + \varepsilon_{\mathbf{k}-\mathbf{q}/2} - \hbar\omega_s(\mathbf{q})} \quad (47)$$

with A, being the unit cell area, which shows that the wave function is purely real, as it should be. Comparing equations (39) and (46) shows that

$$Z^{-1}(\mathbf{q}) = \frac{U^2}{\pi} \sum_{\mathbf{k}} |g_{\mathbf{q}}(\mathbf{k})|^2 = \frac{U^2}{\pi} \int \frac{d^2\mathbf{r}}{A} |\psi_{\mathbf{q}}(\mathbf{r})|^2. \quad (48)$$

Note that we leave C in equation (45) is left undetermined. The normalization is such that $\psi_{\mathbf{q}}(\mathbf{r}=0) = 1$. Equation (48) shows that the intensity of collective mode peaks is a measure of inverse spatial extent of the particle-hole bound state. Smaller particle-hole bound states corresponds to sharper neutron scattering peaks.

[2] Since the free particle-hole basis is composed of Bloch orbitals, therefore the Fourier transform is only an approximation.

References

1. Y. Kopelevich et al., *Studies of High Temperature Superconductors*, Vol. 45, edited by A. Narlikar, S. Moehlecke et al. (Nova Science Publishers, 2003), p. 59; Y. Kopelevich et al., Phys. Rev. B **69**, 134519 (2004)
2. K.S. Novoselov et al., Science **306**, 666 (2004)
3. L. Pauling, *The Nature of The Chemical Bond* (Cornell University Press, 1960)
4. J. Jortner et al., J. Chem. Phys. **42**, 309 (1965)
5. G. Baskaran, S.A. Jafari, Phys. Rev. Lett. **89**, 016402 (2002)
6. A. Goldoni et al., Synthetic Metalas **77**, 189 (1996)
7. S.W. Lovesey, *Theory of Neutron Scattering form Condensed Matter*, Vols. 1 and 2 (Clardon Press, Oxford, 1984)
8. S.W. Lovesey, *Condensed Matter Physics, Dynamic Correlations* (Benjamin/Cummings, Reading, Massachusetts, 1980)
9. A. Murani (private communication)
10. P.R. Wallace, Phys. Rev. **71**, 622 (1947); P.R. Wallace, Phys. Rev. **72**, 258 (1947)
11. R. Saito, G. Dresselhaus, M. Dresselhaus, *Physical Properties of Carbon Nanotubes* (Imperial College Press, London, 1998)
12. S.A. Jafari, Diploma thesis, the Abdus Salam ICTP (2002)
13. N.E. Bickers, D.J. Scalapino, Ann. Phys. **193**, 206 (1989)
14. J. González, F. Guinea, M.A.H. Vozmediano, Phys. Rev. Lett. **77**, 3589 (1996)
15. J. González, F. Guinea, M.A.H. Vozmediano, Nucl. Phys. B **424**, 595 (1994); `cond-mat/0007337`; D.V. Khveshchenko, `cond-mat/0101306`
16. G. Baskaran, S.A. Jafari (to be published)
17. G. Grosso, G. Pastori Parravichini, *Solid State Physics* (Academic Press, 2000)
18. J. Singh, *The dynamics of excitons*, in Solid State Physics, edited by H. Ehrenreich, D. Turnbull, F. Seitz, Vol. 38 (Academic Press, NY, 1984), p. 295
19. N.M.R. Peres et al., Phys. Rev. Lett. **92**, 199701 (2004)
20. G. Baskaran, S.A. Jafari, Phys. Rev. Lett. **92**, 199702 (2004)